NUMERICAL CALCULATION OF AIR VELOCITY AND TEMPERATURE IN ICE RINKS

O. Bellache[1], N. Galanis[1], M. Ouzzane[2], R. Sunyé[2]
[1] Génie mécanique, Université de Sherbrooke, Sherbrooke (QC)
[2] Laboratoire de Recherche en Diversification Énergétique de CANMET, Varennes (QC)

ABSTRACT

The refrigeration load as well as the hydrodynamic and thermal fields in a typical ice rink have been evaluated numerically taking into account heat losses through the envelope. The predictions of different models (laminar forced and mixed convection, turbulent mixed convection) are analysed and compared. They show significant differences in air velocities near the walls and in temperature gradients near the ice. The turbulent mixed convection model gives the best estimate of the refrigeration load.

INTRODUCTION

Canadian ice rinks use approximately 3500 GWh of electricity annually and generate $3x10^5$ tons of gases contributing to the greenhouse effect. The potential for improvement in both areas is substantial. However no concerted effort has been undertaken to develop design procedures and specify operational guidelines which would reduce energy consumption and gas emissions while maintaining the quality of the indoor air and ice as well as the comfort of skaters and spectators. The challenge is great because of the diversity of size and configuration of the buildings, and the differences in heating and ventilation systems in use. This complexity and the coupling between air movement, heat transfer through the building envelope, heat and mass transfer between the air and ice surface, pollutant and water vapour dispersion in a large irregular domain, explain the lack of design and operation norms.

The development of reliable CFD codes offers the potential for systematic analysis of the velocity, temperature and concentration distributions in ice rinks and other large buildings. Several such numerical studies have been undertaken in 2D and 3D configurations [Chen 1990, Chunxin 2000, Nielsen 1974, Whittle 1986]. One of the most significant results has been reported by Chen [1995] who used forced and mixed convection formulations with different turbulence models and found that none is entirely satisfactory for such large buildings. However none of these studies has taken into account heat losses through the building envelope and radiation effects within the building. Furthermore, no CFD study has evaluated systematically the effect of different ventilation and heating systems on energy consumption and ice condition.

In view of this situation, a project aimed to develop a model for ice rinks that takes into account all of the above phenomena and predicts energy consumption as well as ice and comfort conditions has been initiated. This article discusses the predictions of the model developed at the first phase of the project. The results for a typical 2D configuration, which include refrigeration loads as well as heat transfer coefficients between the air and the ice. They also show the effects of heat losses through the ice rink envelope. The predictions of four different formulations are compared and analysed.

FORMULATION OF THE PROBLEM

The present case is based on an actual ice rink in Montreal. It is 33 m wide, 8 m high and 64 m long. Seating for spectators is provided on one of its long sides (figure 1) and two narrow corridors are situated on either side of the ice surface. Ventilation and heating are provided by blowing air towards the seating area from eight regularly spaced inlets situated near the ceiling. In view of this situation, it is considered that a 2D representation of the building is satisfactory.

The partial differential equations modelling the air movement and heat transfer can be written in the following general form :

$$\frac{\partial(\rho\phi)}{\partial t} + \mathrm{div}\left(\rho V \phi - \Gamma\ \mathrm{grad}\,\phi\right) = S \qquad (1)$$

The appropriate values or expressions for ϕ, Γ, and S are defined in Table 1 for each of the cases treated here: laminar forced convection, laminar mixed convection and turbulent mixed convection (using the standard or low-Reynolds number κ-ε models). These equations are non-linear and, in the case of mixed convection, coupled through the buoyancy force. The laminar model is simple but does not take into account the mixing which occurs in the domain. The forced convection model is adequate when heat losses or gains are small, as in spring and autumn [Chen, 1995]. Despite their limitations, these models can provide a

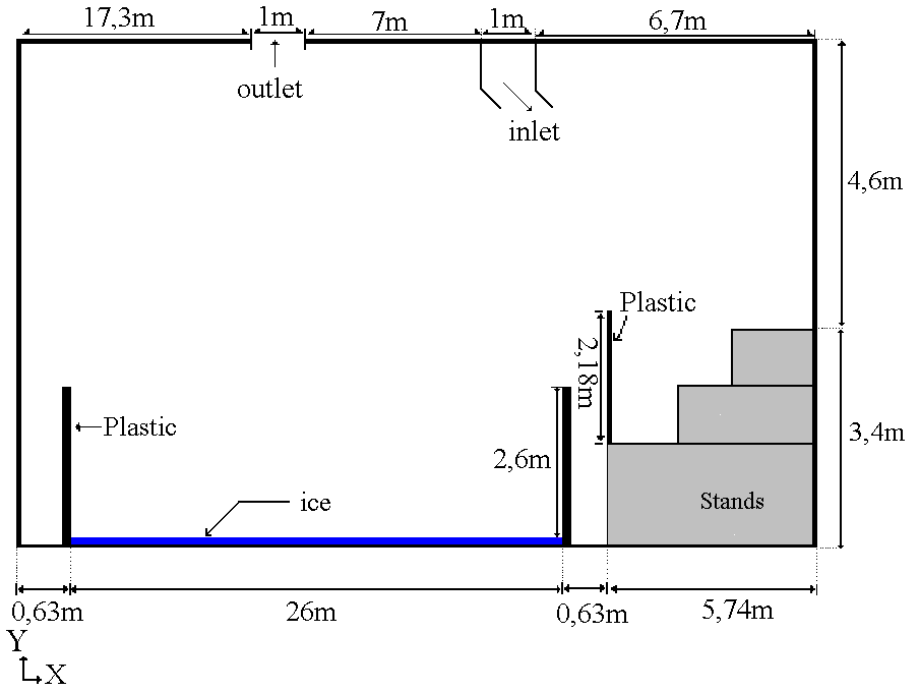

Figure 1. Configuration of ice rink

Table 1. Values of ϕ, Γ and S

Equation	Φ	Γ	S
Mass	1	0	0
X-momentum	U	μ laminar $\mu + \mu_t$ turbulent	$-\partial P/\partial x$ $-\partial P/\partial x$
Y-momentum	V	μ laminar forced μ laminar mixed $\mu + \mu_t$ turbulent mixed	$-\partial P/\partial y$ $-\partial P/\partial y - \rho g\beta(T-T_0)$ $-\partial P/\partial y - \rho g\beta(T-T_0)$
Energy	T	μ/Pr laminar $\mu/Pr + \mu_t/Pr_t$ turbulent	S_T S_T
Turbulent kinetic energy	κ	μ_t/σ_κ standard κ–ε model $\mu + \mu_t/\sigma_\kappa$ low-Re κ–ε model	$G - \rho\varepsilon + G_B$ (standard κ–ε) $G - \rho\varepsilon + G_B$ (low-Re κ–ε)
Dissipation rate	ε	μ_t/σ_ε $\mu + \mu_t/\sigma_\varepsilon$	$[\varepsilon(C_{\varepsilon1}G - C_{\varepsilon2}\rho\varepsilon)/\kappa] + C_{\varepsilon3}G_B(\varepsilon/k)$ $[\varepsilon(C_{\varepsilon1}f_1G - C_{\varepsilon2}\rho f_2\varepsilon)/\kappa] + C_{\varepsilon3}G_B(\varepsilon/k)$

$\mu_t = \rho C_\mu \kappa^2/\varepsilon$ standard κ–ε model
$\mu_t = \rho C_\mu f_\mu \kappa^2/\varepsilon$ low-Re κ–ε model

$f_\mu=(1-e^{-A_\mu R_k})^2(1+A_t/R_t)$; $f_1 = 1 + (A_{c1}/f_\mu)^3$; $f_2=(1-e^{-R_i^2})$
$R_k=(\kappa^{1/2} . dp)/\nu$; $R_t = \kappa^2/\varepsilon\nu$; A_μ=0,0165 ; A_t=20,5 ; A_{c1}= 0,05
$G_B=-g\beta(\mu_t/Pr_t)(\partial T/\partial x_i)$; $G = \mu_t(\partial U_i/\partial x_j + (\partial U_j/\partial x_i).(\partial U_i/\partial x_j)$
$C_{\varepsilon1}$=1,44 ; $C_{\varepsilon2}$=1,92 ; $C_{\varepsilon3}$=1,44 ; C_μ= 0,09 ; σ_κ = 1 ; σ_ε = 1,3

first estimate of the flow and temperature fields with relatively low computing effort. The standard κ–ε model which is only applicable for fully turbulent flows uses wall functions by which the corresponding boundary conditions are transferred to points far from the wall. This is relatively difficult and "lacks theoretical support " [Chen, 1995]. The use of the low-Reynolds number κ–ε model eliminates this problem, but in general increases the computing cost for complex geometries.

The ventilation air enters through a 1 m opening at x = 25,3 m, y = 7,58 m with horizontal and vertical velocities respectively equal to 1,343 m/s and –0,828 m/s. These values correspond to 1760 CFM entering at 60° from the vertical for the entire building. The air leaves through a 1m wide opening in the ceiling (y = 8m) at x = 17,63 m where the static pressure is set equal to 100 kPa. The surface temperature below the ice is –5,5°C while two different conditions have been applied at the walls and ceiling: in the first case they are considered to be adiabatic while in the second they are losing heat by convection (h = 7,4 W/m^2K) to the outside air at T = -22 °C. Although adiabatic envelopes are an idealisation, this condition is included as a limiting case for high insulation levels in order to evaluate the advantages offered by increasing thermal resistance.

NUMERICAL METHOD

The simulations have been carried out with the numerical code PHOENICS [Patankar & Spalding 1972, Spalding 1991] which uses the finite volume method and a staggered grid. The discretisation uses upwind differences in the case of forced laminar convection and hybrid differences in the three other cases. The SIMPLE algorithm [Patankar 1981] is used for the pressure correction and the solution is obtained iteratively starting from an arbitrary initial condition. The discretisation grid is non-uniform. PHOENICS defines a number of zones corresponding to physical discontinuities in the calculation domain (in the present case there are 14 zones in the x direction and 8 in the y direction) and the user selects the number of grid points, or finite volumes, within each resulting subdivision of the domain. For the two laminar cases and the low Reynolds number κ-ε model, a large number of grid points was selected in the zones where important velocity and temperature gradients are expected. On the other hand, in the case of the standard κ-ε model, the PDEs are not applied near the walls and partitions. The variables in the proximity of these solids are obtained from "wall functions" which are integrated in PHOENICS.

Many numerical tests have been executed to ensure that the results are independent of the discretisation grid and the number of iterations. The model and numerical method were validated by comparing the calculated results with experimental values for natural convection of water in a square enclosure with adiabatic horizontal walls and isothermal vertical walls [Cheesewright et al 1986] The results presented here were obtained using more than 90x33 grid points and over 10^4 iterations. The total error for mass, momentum and energy is, in all reported cases, less than 1%.

RESULTS AND DISCUSSION

A good ventilation system must circulate air throughout the building to avoid stagnant areas where air quality deteriorates. However, air velocities must be low, particularly in the vicinity of the stands where the temperature should be near 20 °C. On the other hand, air temperature near the ice must be low to preserve ice quality and to reduce the refrigeration load.

The velocity fields predicted by the previously described four formulations and two boundary conditions have certain common characteristics and some significant differences (some are illustrated in figures 2 and 3). Thus, in all cases the ventilation air flows from the inlet towards the stands, curves downwards and is aspirated towards the outlet. However, the predicted vertical and horizontal penetration of the ventilation air in the domain varies significantly from case to case. Thus, for laminar forced convection it reaches the right hand wall without appreciable vertical displacement, descends towards the stands and then turns towards the exit. On the other hand, the standard κ-ε model with adiabatic walls predicts an almost vertical jet directed from the inlet towards the ice. The laminar forced convection model predicts relatively high velocities near the stands while the corresponding values for the turbulent models are quite low. Most of the models predict a clockwise vortex in the upper half of the domain between the inlet and exit, the only exception being the case of laminar mixed convection with adiabatic walls. In the left half of the domain, all models predict an anti-clockwise vortex. Near the wall, the vertical velocity associated with this movement is more important when heat losses through the envelope are considered. Near the ice, the horizontal velocity is highest in the case of forced laminar convection (approximately 26 cm/s at a distance of 5 cm above the ice). In all other cases the horizontal velocity at this distance from the ice is near 5 cm/s.

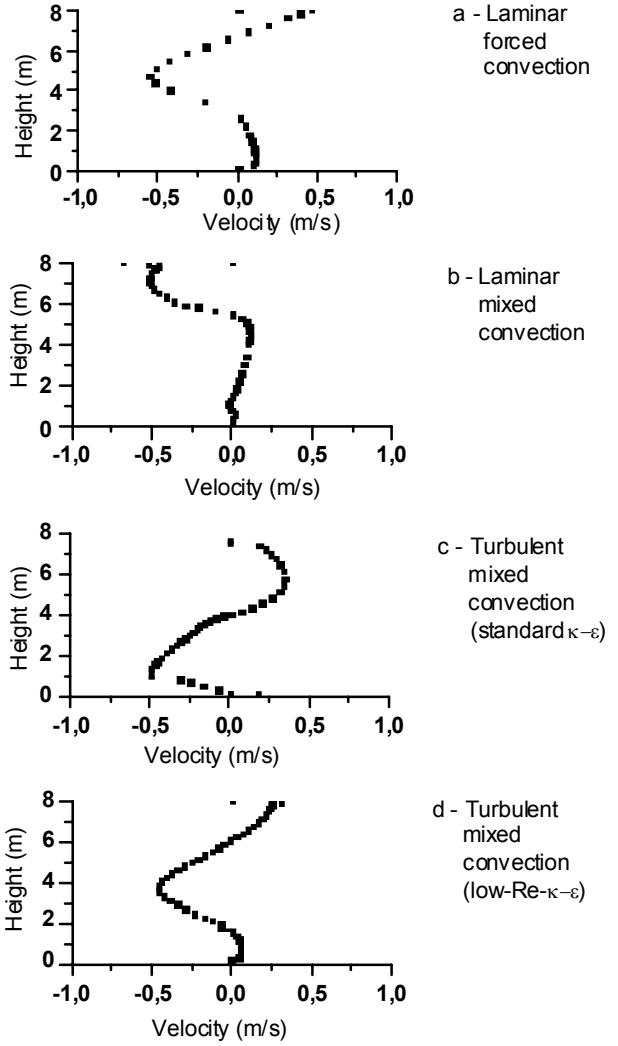

Figure 2. Profiles of horizontal component of velocity at x = 22 m (adiabatic walls)

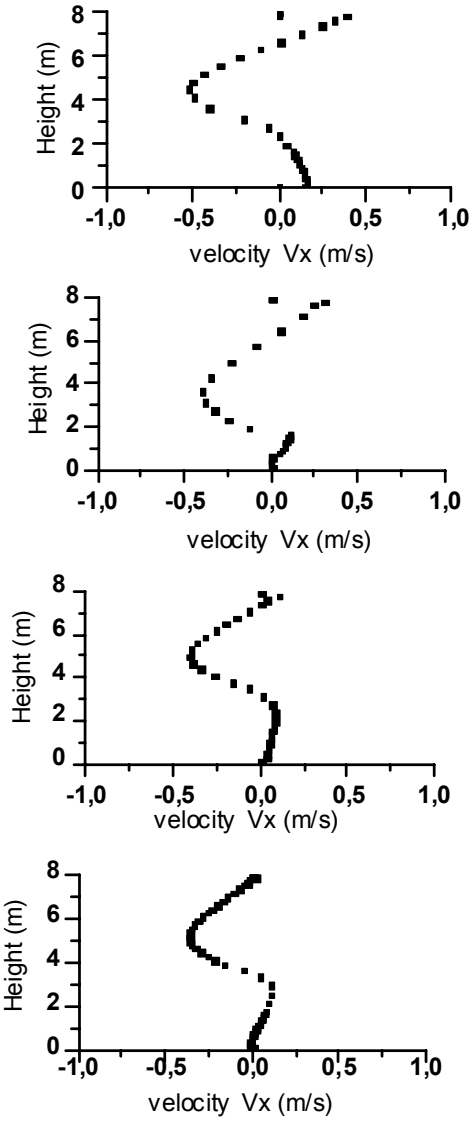

Figure 3. Profiles of horizontal component of velocity at x = 22 m (non-adiabatic walls)

The air temperature in a large part of the domain is essentially equal to the imposed value at the air inlet. The surface temperature of the ice never exceeds -4°C. Over the ice, a thermal boundary layer is formed in which the air temperature increases with y. The vertical profile of the temperature (figures 4 and 5) is essentially independent of x but is quite different from case to case. In general the air temperature near the ice (at y = 0.2 m) is lower when heat losses through the walls and ceiling are not considered. The predicted temperatures for the adiabatic envelopes are uniform outside the thermal boundary layer for the two laminar and the standard κ-ε models.

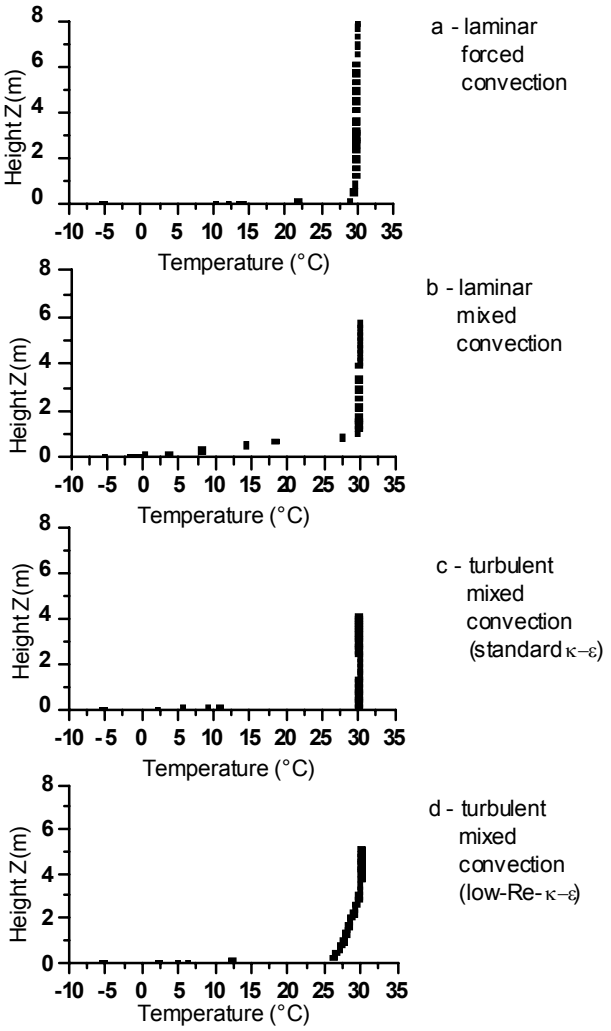

Figure 4. Temperature profiles at x = 26 m (adiabatic walls)

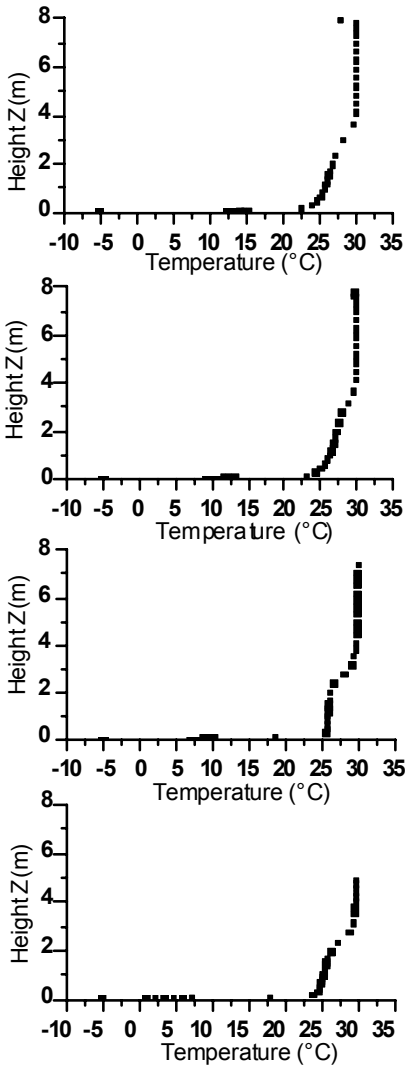

Figure 5. Temperature profiles at x = 26 m (non-adiabatic walls)

On the other hand, for the low-Reynolds κ-ε model the temperature profile exhibits two regions of temperature variation with very different gradients. When heat losses are considered, the temperature profiles show an increase of the gradient at approximately y = 3 m. This is attributed to the ventilation jet which does not penetrate to lower heights due to the presence of the stands. Unfortunately, corresponding experimental results are not available yet so that it is impossible to choose the most accurate model based on such profiles.

The effect of heat losses on the air temperature near the ice is important in the case of the two laminar and of the standard κ-ε formulation but negligible in the case of the low-Reynolds κ-ε formulation. It is interesting to note the significant decrease of the ceiling temperature when heat losses are considered. This decrease varies from as little as 3 °C in the case of laminar forced convection to as much as 25 °C in case of laminar mixed convection.

Table 2 Energy fluxes and convection coefficients

	1. Forced laminar	2. Mixed laminar	3. Mixed turbulent (standard κ-ε)	4. Mixed turbulent (low-Re κ-ε)
	A. Adiabatic walls and ceiling			
Thickness of thermal boundary layer (m)	-	0,5	0,05	0,06
h_1 (W/m^2 °C)	-	0,05	0,49	0,47
h_2 (W/m^2 °C)	0,13	0,07	0,09	0,09
Refrigeration load (W/m)	237	32	129	218
Lack of closure in energy balance - W/m - % of inlet energy	 13 0,005	 50 0,02	 166 0,06	 97 0,03
	B. Wall and ceiling with heat losses			
Thickness of thermal boundary layer (m)	0,14	0,3	0,09	0,1
h_1 (W/m^2 °C)	0,18	0,08	0,29	0,26
h_2 (W/m^2 °C)	0,15	0,05	0,04	0,14
Refrigeration load (W/m)	166	32	178	194
Heat losses (W/m)	96	229	1126	1113
Lack of closure in energy balance - W/m - % of inlet energy	 140 0,05	 8 0,003	 45 0,02	 40 0,02

The corresponding values for the two turbulent formulations are approximately 10 °C. Similar difference were observed in the case of the vertical wall temperatures. The difference between the temperatures of the surfaces surrounding the domain will of course be attenuated if radiation exchanges are considered. This effect will be included in the next phase of the project.

Table 2 presents estimates of the thermal boundary layer thickness H based on the previously discussed air temperature profiles. Carling [2000], used this thickness to estimate the temperature gradient in the air and obtained the heat transfer coefficient between the ice and air from :

A second estimate of this coefficient can be evaluated

$$h_1 = \frac{k_{air}\left(T_{air} - T_{ice}\right)}{H\left(T_{air} - T_{ice}\right)} = \frac{k_{air}}{H} \qquad (2)$$

by expressing the air temperature gradient near the ice in terms of the air temperature at the grid points closest to the ice. Thus, using a Taylor expansion :

$$\frac{\partial T}{\partial Z} = \frac{8T_{ice} - 9T_{a1} + T_{a2}}{3\left(\Delta Z\right)} \qquad (3)$$

$$h_2 = \frac{k_{air}}{T_{air} - T_{ice}} \frac{8T_{ice} - 9T_{ai} + T_{a2}}{3(\Delta Z)} \qquad (4)$$

The values of h obtained with these two expressions are quite different, especially for turbulent flow. In general, equation 2 gives higher estimates while equation 4 gives estimates which are close to the thermal conductivity of air. Since the velocities near the ice are quite small and the thermal boundary layer thickness is difficult to estimate with precision, we believe that the values obtained from equation 4 are more reliable. Finally, Table 2 also presents calculated values of the refrigeration load Q_g and of the heat losses Q_L through the envelope. The values of Qg with heat losses are quite different from those for an adiabatic envelope. Even more significant is the variation of both Qg and Q_L from one formulation to another. It should be noted however that, in some cases (2A, 3A and 1B of table 2) the values of Q_g and Q_L are of the same order of magnitude as the lack of closure of the global energy balance. In those three cases the values of these two heat fluxes are therefore not reliable even though the lack of closure represents a negligible percentage of the incoming energy. These observations indicate that CFD codes should be used with caution when evaluating heat fluxes across the boundaries of large domains.

The refrigeration load and the heat losses were also calculated using a global energy balance with constant convection coefficients (0,27 , 0,17 and 0,14 W/m^2K for heat transfer between the air and ice, across the walls and across the ceiling respectively). The corresponding results are Q_L = 1188 W/m and Q_g = 232 W/m. These values are comparable to the predictions of the two turbulent models with non adiabatic walls and ceiling.

CONCLUSION

Numerical simulation of the hydrodynamic and thermal fields in an ice rink has been carried out using a commercial CFD code. The complexity of the geometry has been taken into account by considering such elements as plastic protection panels which have a significant effect on the flow field. Heat losses through the walls, ceiling and the ice have also been taken into account and, therefore, estimates of the refrigeration load have been established. These simulations are considered successful from a numerical point of view since convergence and closure have been attained.

The prediction of the mean velocity field by the four models is qualitatively similar. However velocity component near the walls and ceiling as well as temperature gradients near the ice differ significantly. Based on these observations and the values of the refrigeration load and heat losses we consider that the mixed convection turbulent model is the most appropriate. The standard κ–ε formulation is very stable and requires less computing effort than the low-Reynolds number one. On the other hand, the latter does not use the empirical wall functions. The choice between these two formulations will be based on an upcoming experimental validation of their predictions.

NOMENCLATURE

$C_{\varepsilon 1}$, $C_{\varepsilon 2}$, $C_{\varepsilon 3}$, C_μ	turbulence model constants
f_1, f_2, f_μ	turbulence model functions
g	gravity
G_B	buoyancy production of κ
G	stress production of κ
h	convection coefficient
k_{ai}	thermal conductivity of air
P	static pressure
Pr_t	turbulent Prandtl number
Q_g	refrigeration load
Q_L	heat losses
T	temperature
t	time
U.V	components of velocity
S	source term
β	expansion coefficient
Γ	diffusion coefficient
ε	turbulence dissipation rate
κ	kinetic energy of turbulence
μ	dynamic fluid viscosity
ν	kinetic fluid viscosity
ρ	density
σ_t, σ_ε, σ_κ	turbulence model constants
ϕ	general field variable

REFERENCES

Cheesewright R. , King K.J. and Ziai S. (1986), Experimental data for validation of computer codes for the prediction of two-dimensional buoyant cavity flows, Significant questions in buoyancy affected enclosure or cavity flows, ed: Humphrey, J.A.C., et al., New York: ASME, 75-81.

Chen Q. , Moser A. and Huber A. (1990), Prediction of buoyant, turbulent flow by a low-Reynolds-number κ–ε model, ASHRAE Transactions, 96 (1), 564-573.

Chen Q. (1995), Comparison of different κ–ε models for indoor air flow computations, Numerical Heat Transfer, Part B, 28, 353-369.

Chunxin Y. , Demokritou P. and Chen Q. (2000), Ventilation and air quality in indoor ice skating arenas, ASHRAE Transactions, 106 (2), 338-346.

Nielsen P.V. (1974), Flow in air conditioned rooms, Ph.D. Thesis, Technical University of Denmark.

Par Carling M. (2000), Physical processes in ice rinks studied with small scale modelling, ROOMVENT'2000.

Patankar S.V. (1980), Numerical heat transfer and fluid flow, Mac Graw Hill Book Co. ,New York . Patankar S.V. and Spalding D.B. (1972), A calculation procedure for heat, mass and momentum transfer in three-dimensional parabolic flows, Int. J. Heat Mass Transfer, 15, 1787-1805.

Spalding D.B. (1991), The Phoenics reference manual, CHAM TR/200a (PIL), TR/200b (FORTRAN).

Whitlle G.E. (1986), Computation of air movement and convective heat transfer within buildings, Int J. of Ambient Energy, 7(3), 151-164.